Chemical Engineering Journal 517 (2025) 164562

Contents lists available at ScienceDirect

Chemical Engineering Journal

journal homepage: www.elsevier.com/locate/cej

Proof of concept for a sorption-enhanced reactor with continuous sorbent feeding (CSF): application to green methanol production☆

R. González-Pizarro, J. Lasobras, J. Soler *, J. Herguido, M. Menéndez

Aragon Institute of Engineering Research (I3A) - Catalysis and Reactor Engineering Group (CREG), Universidad de Zaragoza, C/ Mariano Esquillor s/n, 50018 Zaragoza, Spain

ARTICLE INFO

Keywords:
Process intensification
Sorption enhanced reaction
Green methanol
E-fuels

ABSTRACT

A new reactor for process intensification using sorption enhanced reaction is described. The novelty compared with most experimental work is that a continuous sorbent feeding (CSF) provides a steady state operation. The sorbent increases the reaction rate of a reversible reaction. The reactor is based on the phenomena of segregation of solids in fluidized bed reactors by using a catalyst and a sorbent. Under certain conditions of density and particle size, the two solids segregate and the sorbent may be removed from the bed with only a small content of catalyst. The system has been experimentally tested in the hydrogenation of CO_2 to methanol, using a zeolite as sorbent. A significant increase in CO_2 conversion was achieved compared with the same reactor without sorbent.

1. Introduction

Fuels produced from CO_2 and green hydrogen (i.e., hydrogen from solar or wind energy), are a promising way to solve several of the main societal challenges [1–3]: a) increasing CO_2 emission [4], b) depletion of fossil fuels, c) difficulties in the decarbonization of some transport sectors [5,6], d) intermittency of renewable resources, and e) security of energy sources. Fuels from CO_2 and renewable energy, commonly named as e-fuels, include methanol, dimethyl-ether and methane (also known as Renewable Natural Gas), and hydrocarbons obtained by Fischer-Tropsch.

The corresponding reactions may be written as follows:

$$CO_2 + 3\,H_2 \rightleftharpoons CH_3OH + H_2O \quad (1)$$

$$CO_2 + 6\,H_2 \rightleftharpoons CH_3 - o - CH_3 + 3\,H_2O \quad (2)$$

$$CO_2 + 4\,H_2 \rightleftharpoons CH_4 + 2\,H_2O \quad (3)$$

$$nCO_2 + 3n\,H_2 \rightarrow (CH_2)_n + 2n\,H_2O \quad (4)$$

All the above reactions share a common characteristic: water is produced in the process, in some cases even more moles of water than moles of the desired product. In the first three cases (methanol, dimethyl-ether and methane) the reaction yield is limited by the thermodynamic equilibrium. Therefore, removing water and intensifying the process, it is possible to achieve yields higher than those obtained under non-intensified conditions. This improvement is due to the removal of water formed during the reactions, which shifts the thermodynamic equilibrium toward product formation—an effect that does not occur in conventional processes [7]. In the case of Fischer-Tropsch synthesis, water removal may also provide increases in reaction rate and other advantages [8].

The same idea can be applied to the Reverse Water Gas Shift reaction, that can be employed as an intermediate step in all the processes for the transformation of CO_2 to other products:

$$CO_2 + H_2 \rightleftharpoons CO + H_2O \quad (5)$$

The removal of water from the catalyst environment may be obtained by means of a membrane (i.e., using a membrane reactor) or using a sorbent selective to water (a case of the so-called Sorption Enhanced Reactor). Membrane reactors have been studied for methanol, dimethyl-ether and Fischer-Tropsch reaction [9–18]. In the last case the target is not to change the equilibrium but to avoid undesirable effects of water on the reaction rate or on the catalyst stability. Membrane reactors that remove water are usually based on zeolite membranes, and several works have described its performance by simulations or from experimental laboratory experiments. Many reviews have provided a wide overview of the achievements in the field of zeolite membrane reactors [19–21]. The feasibility of using carbon-molecular sieve

☆ This article is part of a Special issue entitled: 'ISCRE 28' published in Chemical Engineering Journal.

* Corresponding author.
E-mail address: jsoler@unizar.es (J. Soler).

https://doi.org/10.1016/j.cej.2025.164562
Received 17 January 2025; Received in revised form 4 June 2025; Accepted 5 June 2025
Available online 6 June 2025

Nomenclature

SER	sorption enhanced reaction
CSF	continuous sorbent feeding
rWGS	reverse water gas shift
GHSV	gas hour space velocity
U_{mf}	minimum fluidization velocity
U_r	reduced velocity
LTA	Linde type A
TOS	time on stream
ΔP	pressure drop

membranes has been disclosed in recent works [22,23]. Sorption Enhanced Reaction (*SER*) is another technology that is included in the broad field of Process Intensification. SER aims to increase the reaction rate and the achievable yield by using a sorbent. In most experimental published works the sorbent is located in a fixed bed, together with the catalyst [24–32]. Those experiments show that the sorbent becomes saturated after a few minutes and therefore the reactor must operate in cycles of reaction and regeneration, i.e., in non-steady state. Kuczynski et al. [33] employed a fixed-moving bed reactor, where the sorbent was moving through the free spaces of a fixed bed of catalyst. The experimental results, showing conversions higher than those of the thermodynamic equilibrium, were in good agreement with the results from a mathematical model [33]. Coppola et al. [34] proposed a dual fluidized bed, where the solids would circulate between a reactor and regenerator, although in their experimental system the solid was operating also in cycles, i.e., in non-steady state.

A recent work [35] has disclosed a proposal for a *SER* with continuous feeding and removal of sorbent that allows steady state operation. In addition, the continuous sorbent feeding (CSF), separating it from the reactor with a low content of catalyst particles, would avoid the heating of the catalyst during the sorbent regeneration step, which may easily contribute to its deactivation. This new reactor is based on a fluidized bed containing a binary mixture of solids, i.e., catalyst and sorbent, with different size and/or density, in such a way that the two solids will segregate, and it will be possible to remove the sorbent from the point where the concentration of catalyst is low. This is exemplified in Fig. 1, where the catalyst is acting as jetsam (i.e., it tends to fall to the bottom of the bed) and the sorbent is the flotsam (i.e., it raises to the top of the bed). The objective of this work is to check experimentally the feasibility of this reactor configuration. In particular it will be applied to the hydrogenation of CO_2 to methanol.

2. Experimental

2.1. Solid preparation

2.1.1. Preparation of catalyst

In_2O_3/ZrO_2 catalyst was selected due to its good properties in the methanol synthesis reaction: i) high mechanical strength which allow using it in a fluidized bed for long time on stream, ii) possibility to work at a high temperature and iii) high selectivity toward methanol.

The catalyst was synthesized via wet impregnation method, following the procedure described in the literature [36], with the only modification being a 50 % reduction in the solvent volume. Specifically, 2.36 g of $In_2(NO_3)_3{\cdot}xH_2O$ (99.99 %, Sigma Aldrich) and 9.1 g of monoclinic ZrO_2 (ThermoScientific) were added to a solution of 217.5 mL ethanol and 93.2 mL water (70/30 % *v*/v ethanol/water). The mixture was stirred at 150 rpm for 12 h, after which the solvent was evaporated at 60 °C using a (*Buchi*) rotary evaporator. Calcination was carried out in two steps: 2 h at 100 °C and then 2 h at 500 °C, both with a ramp rate of 2 °C/min. The final catalyst was sieved to obtain particles in the desired size range.

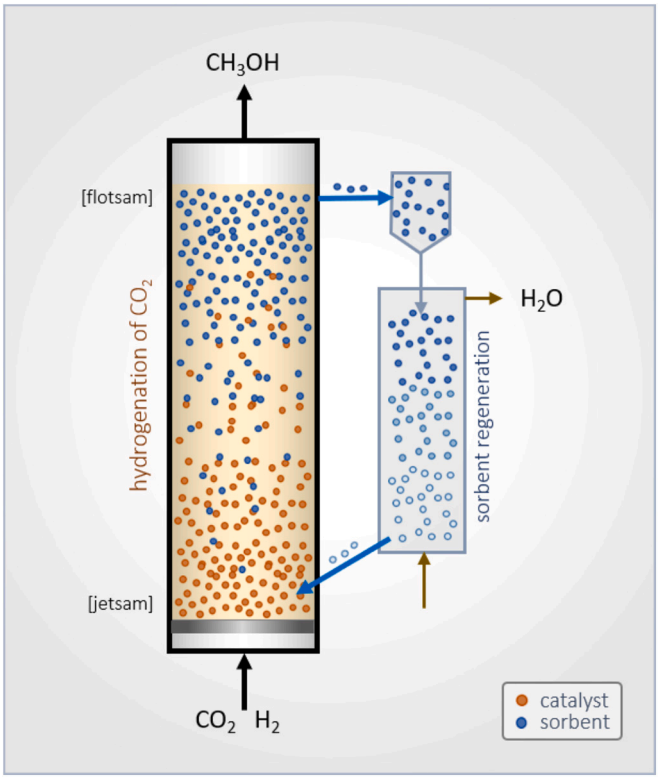

Fig. 1. Scheme of the proposed setup for methanol synthesis with a *SER* with continuous feeding and removal of sorbent.

2.1.2. Preparation of zeolite

3A zeolite, provided by *Thermofisher Scientific* was used as a sorbent for this study. To achieve the particle size required, between 75 and 150 μm, it was ground from 3 to 4 mm spheres and sieved. This selection allows for selective segregation, as the two solids used differ in both size and density. In this process, zeolite is the lighter and smaller solid ("flotsam"), enabling its separation into the upper region of the bed through segregation.

Zeolite 3A it was chosen because, being an LTA zeolite, it is characterized by its low Si/Al ratio, which indicates high hydrophilicity, meaning a strong affinity for water adsorption. Additionally, this sorbent has a small pore size, <3 Å, making it highly selective for water adsorption.

2.2. Reactor

Fig. 2 presents the design of the fluidized bed reactor with continuous sorbent feeding (CSF), catalyst in color red and sorbent in blue. This non-conventional fluidized bed reactor is constructed from stainless steel and has an internal diameter of 3 cm. It includes standard gas inlet and outlet ports, similar to those of a conventional fluidized bed reactor, with a total length of 24 cm. In addition, it features two lateral ports (a lower lateral inlet and an upper lateral outlet) designed specifically for the continuous feeding and removal of solid material. The reactor is equipped with three inlets and two outlets, depending on the type of feed (gas or solid). Regarding gas-phase feeding, the reactor includes two inlets: the first is located at the bottom of the reactor, acting as the conventional gas inlet; the second is positioned at the lower lateral port and is used to introduce a nitrogen stream that facilitates the *CSF*. The gas outlet is located at the top of the reactor and allows for the complete discharge of the gaseous flow passing through the system. For solid-phase feeding, the reactor has one inlet and one outlet. The solid is

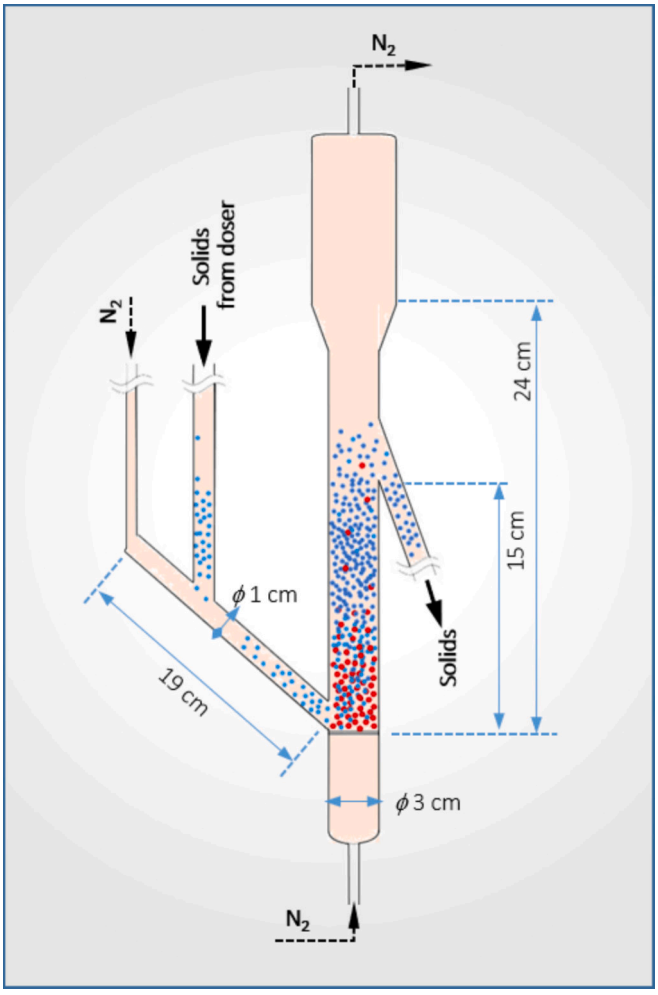

Fig. 2. Scheme of the reactor.

introduced through the lower lateral inlet, carried by the auxiliary nitrogen flow to prevent clogging or backflow. The outlet of solid is located at the upper lateral port, positioned 15 cm above the porous distributor plate. Its purpose is to maintain a fixed bed height; when the bed level reaches this outlet, the solid at the top of the bed overflows into the collection vessel (overflow tank), ensuring continuous removal.

The theoretical basis of this novel process lies in the combination of Sorption Enhanced Reaction (SER) and the segregation of a binary solid mixture. The Sorption Enhanced Reaction concept involves the use of a sorbent solid that selectively removes a reaction product, thereby shifting the reaction kinetics toward increased product formation and enhancing process intensification. The main limitation of this approach is the finite adsorption capacity of the solid sorbent. Once saturation is reached, the sorbent behaves as an inert material and no longer contributes to intensification. The second key principle is the segregation of binary solid mixtures. This is based on the selective spatial separation of two solids within a fluidized bed reactor, governed by differences in physical properties such as particle size, density, and minimum fluidization velocity. The solid with greater size and density—and consequently, a higher minimum fluidization velocity—accumulates in the lower region of the bed, referred to as the "jetsam." In contrast, the lighter solid with smaller particle size and lower minimum fluidization velocity migrates to the upper region, known as the "flotsam".

The segregation occurring inside the fluidized bed reactor refers to the separation between the catalyst and the sorbent, a concept originally introduced by Nienow et al. [37] In our system, the catalyst remains in the lower region of the bed (the "jetsam"), while the sorbent accumulates in the upper region (the "flotsam").

2.3. Experimental system

Fig. 3 shows the experimental setup. It consists of a stainless-steel reactor housed inside an electric furnace. The fluidized bed is supported by a porous plate, acting as gas distributor. The reactor geometry is detailed in Fig. 3. Reactants are fed into the system using mass flow controllers (Alicat Scientific and Brooks). The reactor outlet gas stream is heat-traced and maintained at 180 °C up to the condenser to prevent premature condensation of products such as H_2O or CH_3OH within the piping.

Upon reaching the condenser, condensable compounds (e.g., H_2O and CH_3OH) are condensed and collected for subsequent analysis. Condensation is carried out using an ice-salt bath at −15 °C to prevent damage to the pressure control valve and the gas chromatograph. Once the condensable gases are removed, the remaining gas stream passes through the pressure control valve and is directed either to an online gas chromatograph (CP-3800, Varian, equipped with a molsieve column) for analysis or to a bubble flow meter. Reactor pressure is regulated via a pressure controller (Equilibar). In addition, the system includes two pressure indicators: one at the gas inlet and another at the solids inlet. Gas-phase compounds are monitored continuously using the online gas chromatograph. In contrast, liquid-phase compounds are analyzed at the end of the experiment; by a GC–MS (GC–MS QP2010, Shimadzu) equipped with a capillary column (TRB-50.2 PONA, Teknokroma).

Since the dispenser operated at atmospheric pressure and the reactor was at higher pressure, they cannot be connected directly. A set of two automatic ball valves was employed to separate them, with a repository between them. The dispenser, contains the sorbent and distributes the solid at a constant flow rate of 3 or 4.5 $g_{sorbent}$/min. Two additional valves connected the repository with an inert gas at the same pressure than the reactor and with the atmosphere, in order to keep it at a suitable pressure at each moment. The solids dispenser was a *Lambda doser* model. It has a capacity of 3 L and can add the solid at a flowrate of up to 13.7 g/min.

The operation of the four valves may be divided into two directions: horizontal (for gas supply, pressurizing, or depressurizing the repository) and vertical (for sorbent addition, filling, or emptying the cavity of sorbent). This system operates cyclically. Initially, the repository was empty and at atmospheric pressure. The valve connecting the repository to the dispenser was opened to fill it with sorbent. Once filled, the valve is closed. Next, the gas supply valve was opened to pressurize the cavity to the operating pressure of the reactor; once this pressure is reached, the valve was closed. With the repository filled with sorbent and pressurized, the valve connecting this cavity to the reactor solid entry point was opened. By the effect of gravity, the solid enters the reactor. Once the repository was emptied of sorbent, the valve was closed, and the gas venting valve was opened to depressurize the repository, returning to the initial conditions for a new sorbent feeding cycle. The operation of the valves was automated and he total time for each cycle was 70 s.

30 g of catalyst were loaded in the reactor and heated in an inert atmosphere. When the catalytic bed reached 300 °C, the catalyst was activated in Ar at 0.5 MPa for 1 h. Then, the oven temperature was lowered to the reaction temperature and pressure was set at the desired value. After this, reaction gases were fed to the reactor. In the experiments with sorbent addition, the operation of the sorbent doser started five minutes later. At the same time, valves that control the solid addition were activated. The gas samples were analyzed every fifteen minutes. When the experiment was finished, the liquid sample was analyzed by GC–MS. The conversion calculus was carried out with the Eq. (6), being $F_i^{in/out}$ = inlet/outlet molar flow of substance i (mmol/min) and a mean value was employed for the methanol flow.

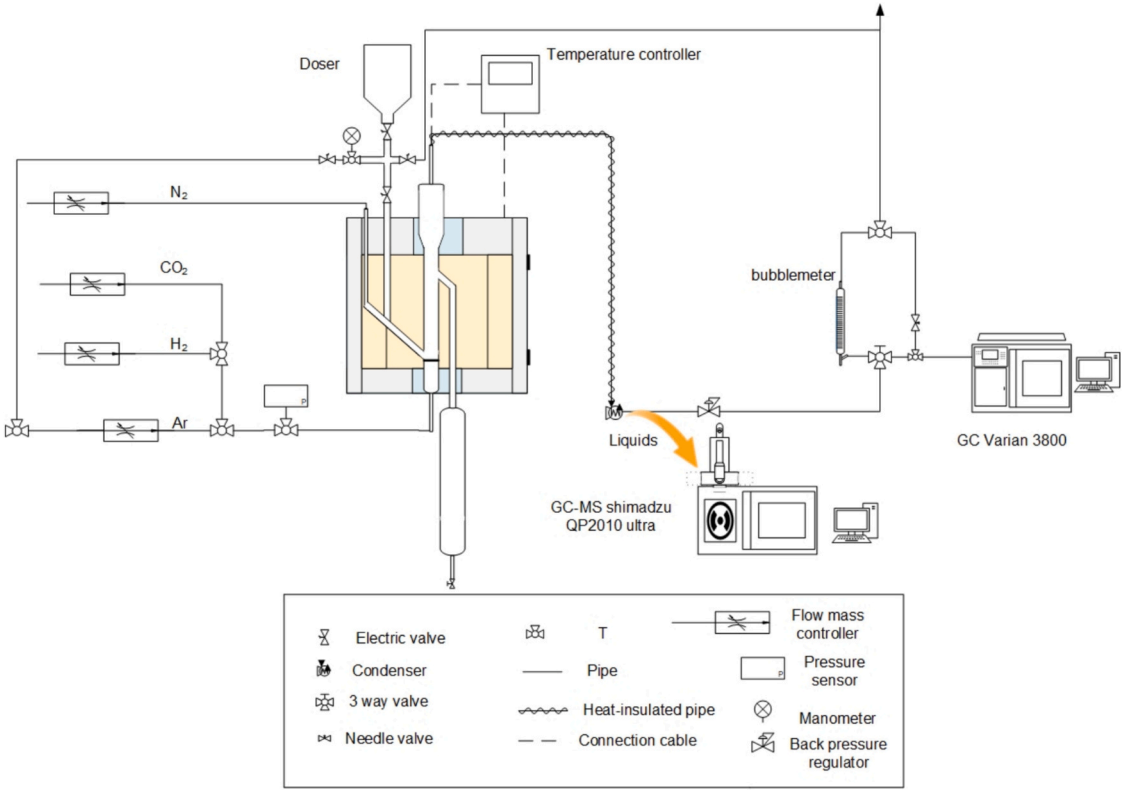

Fig. 3. Scheme of the experimental plant.

$$X_{CO_2} = \frac{F^{out}{}_{CO} + F^{out}{}_{methanol}}{F^{in}{}_{CO_2}} \quad (6)$$

The operating conditions used in the reaction tests are shown in Table 1. Although methanol synthesis is typically carried out at pressures higher than atmospheric, this study was conducted mainly at an atmospheric pressure. As a result, the products formed will predominantly originate from the Reverse Water Gas Shift (RWGS) reaction (5). This reaction produces H_2O as a product, which is consequently intensified by water adsorption (Sorption-Enhanced Reactor).

3. Results

3.1. Solid characterization

The characterization of the solids included BET, XRF, and XRD analyses. BET measurements were performed using a Quantachrome® Autosorb iQ3 device. The XRF analysis was made with a Thermo Fisher Scientific X-ray fluorescence spectrometer from the PERFORM series, equipped with a Rhodium (Rh) X-ray tube. The UNIQUANT software was used for semi-quantitative, patternless analysis (sequential analysis from F to U). XRD measurements were carried out with an X-ray diffractometer with a rotating anode (*RIGAKU Ru2500*). The diffractometer operated at 40 kV and 80 mA, with a Cu anode and a graphite monochromator to select K_α radiation. Measurement conditions were set from $2\theta = 5°$ to 70°, with a step size of 0.03° and a time of 1 s per step. The pore diameter was estimated using the BJH method.

Both solids were characterized before and after use in 19 cycles of adsorption-regeneration to evaluate their degradation (Table 2 and Table 3).

From the values obtained it can be seen that both catalyst and sorbent keep the chemical and textural properties after experiments.

Fig. 4 shows the XRD patterns of both the fresh zeolite and the zeolite used in 19 cycles of experiment/reaction-regeneration. It can be observed that both patterns are identical, indicating that the crystalline structure of the zeolite has not been affected after the 19 cycles, as expected, since these zeolites exhibit a longer lifespan [30,31].

Table 1
Operating conditions in reaction tests.

	Reference value	Interval
Bed temperature, T (°C)	250	250–275
Catalyst particle size, d_p (μm)	[160–200]	
Pressure, P (atm)	1	1–20
CO_2/H_2 ratio (−)	1/3	
Relative gas velocity, $u_r = u/u_{mf}$ (−)	1.5	
Gas hourly space velocity, $GHSV$ (h^{-1})	1250	1250–18,100
Sorbent mass flowrate, m_s (g. min^{-1})	3	

3.2. Segregation tests

To study the fluidization properties of the solids, a test was carried out on each of them, where the pressure drop ΔP of the bed was measured vs flow rate of a nitrogen stream fed using an *Alicat Scientific*® flow meter-controller at laboratory conditions [36]. The minimum fluidization velocity (u_{mf}) was calculated following the correction described by Renda et al. [38], both the operating temperature T and pressure P were modified in the relation to the laboratory conditions, as well as the feed gas, changing from the N_2 used for studying the ΔP to the gas mixture employed ($CO_2 + H_2$). The correct segregation of the solids in the bed was experimentally validated in a previous study [35]. The system consisted of a fluidized bed reactor in which a solids binary

Table 2
In_2O_3/ZrO_2 BET and XRF results for fresh and used samples.

In_2O_3/ZrO_2	In (%wt)	SA_{BET} (m^2/g)	d_p (nm)
Fresh	7.21	90	2.6
Used	7.18	92	2.6

Table 3
Zeolite 3A BET and XRF results for fresh and used samples.

Zeolite 3A	Al (%wt)	K (%wt)	Si/Al	SA_{BET} (m^2/g)	d_p (nm)
Fresh	14.27	14.50	1.28	38.2	1.6
Used	14.27	13.90	1.26	23.6	1.6

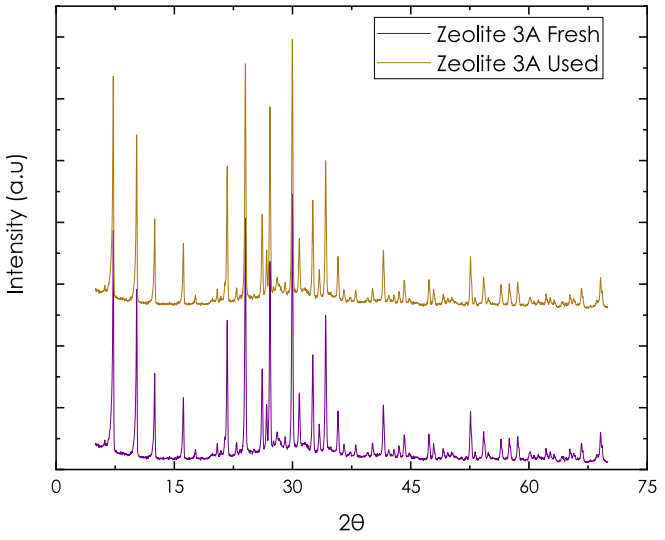

Fig. 4. XRD patterns: (a) Fresh Zeolite 3A, (b) Used Zeolite 3A.

mixture was introduced: i) a catalyst for methanol synthesis, and ii) a sorbent capable of adsorbing water, in order to shift the reaction toward the formation of products.

Additionally, to check the losses by attrition and elutriation, tests were carried out in which the solids were subjected to a high air flow for a prolonged period of time (3 h). It was observed that the catalyst losses were 1.5 wt%/h, while for the zeolite it was 3 wt%/h, which is consistent with a lower mechanical resistance of the zeolite.

The segregation tests were conducted using a quartz reactor with identical dimensions and geometry to that used in the atmospheric condition experiments. Once the segregation test was completed, the solid mixture inside the reactor was extracted using a suction rod connected to a vacuum pump. The bed was sampled in 1 cm-thick sections along the reactor height, in order to analyze the longitudinal profile of the mass fractions of each solid within the bed. Each section was analyzed by sieving the solid mixture. Since the catalyst particles are larger than the zeolite particles, complete separation was achieved, allowing for accurate determination of the mass percentage of each solid in each section.

Several experiments to validate the segregation with different operational conditions were carried out. The first studied parameter was the catalyst amount loaded in the reactor. The N_2 flow rate added by the bottom was 1460 mL (STP) /min and 60 mL (STP) /min by the lateral inlet (Fig. 2). As it can be seen in Fig. 5, for a zeolite addition flowrate of 3 g/min a good segregation profile in steady state is achieved for both situations (i.e., with 30 and 50 g catalyst loads).

As anticipated, by increasing the amount of catalyst load in the catalytic bed (Fig. 5.B) the segregation occurs at higher regions of the reactor. Since the reactor size is fixed, an increase in the total catalyst mass leads to this solid occupying a larger volume within the reactor, thus expanding the jetsam-rich zone.

To prove the influence of catalyst size, two additional experiments were done with catalyst size in the interval 160–200 μm with different N_2 flow rates: 900 mL (STP) /min through the porous plate plus 55 mL (STP)/min by the lateral tube in one case and 1000 mL (STP)/min plus 60 mL(STP)/min, in the other case. A good segregation was also

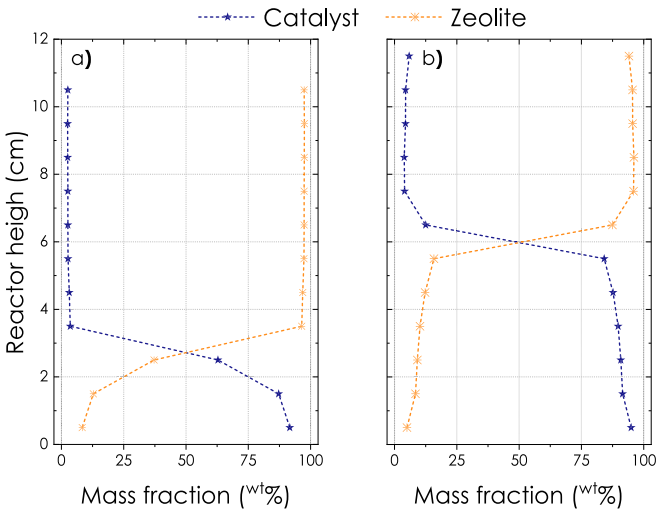

Fig. 5. Segregation tests with different catalysts loadings using catalyst size between 200 and 250 μm: (a) 30 g and (b) 50 g $u_r = 1.5$.

obtained (Fig. 6).

When studying the relative velocity ($u_r = u/u_{mf}$), it can be observed that a higher volumetric feed flow rate, and consequently a higher relative velocity, results in worse segregation. This is because high gas velocity increases the mixing effect of bubbles and because the catalyst (jetsam) experiences a greater expansion, reaching higher bed heights as a result. A parallel work has studied the effect of operating conditions on the segregation [25] showing that there is an optimum value of gas velocity that maximizes segregation.

3.3. Reaction tests

Fig. 7 shows the influence of the continuous addition of an sorbent in CO_2 hydrogenation for two different temperatures ($T = 250$ °C and $T = 275$ °C) and without sorbent addition and with sorbent addition, two mass flowrates were studied ($m_s = 3$ g/min and $m_s = 5$ g/min) of zeolite 3A as added sorbent solid. The remaining operating conditions are those indicated in Table 1 as reference values.

Fig. 7 shows the catalytic activity of In_2O_3/ZrO_2 in a fluidized bed reactor, both in the absence of zeolite and under intensified conditions

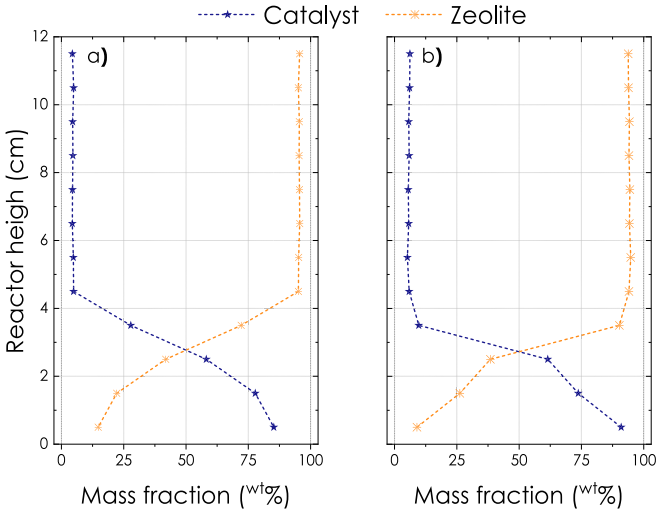

Fig. 6. Segregation tests with different flow rates using catalyst size between 160 and 200 μm: (a) 900 mL(STP)/min through the porous plate plus 55 mL (STP)/min by the lateral tube and (b) 1000 mL(STP)/min through the porous plate plus 60 mL(STP)/min by the lateral tube.

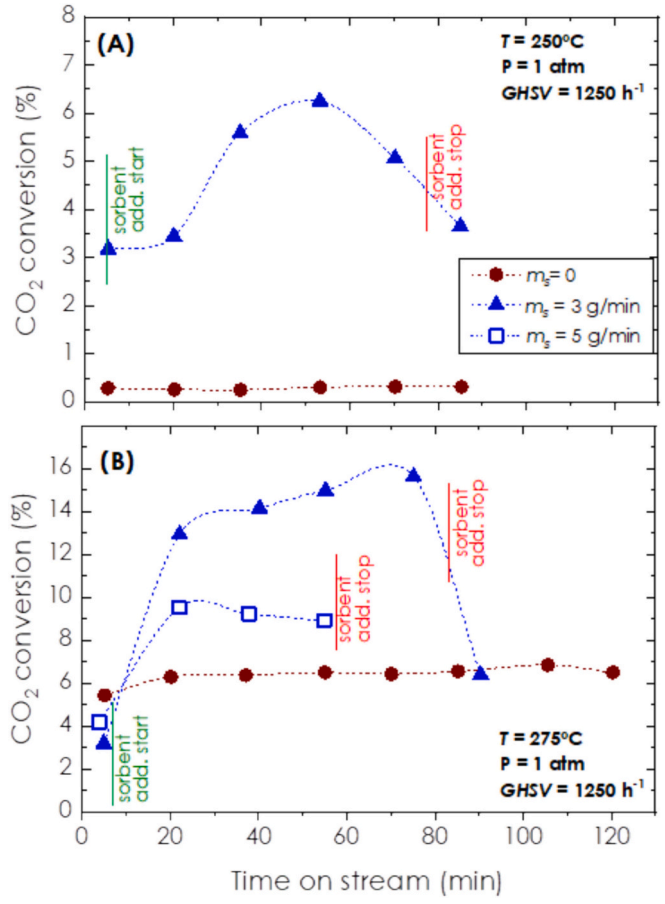

Fig. 7. CO_2 conversion as a function of time-on-stream, with ($m_s = 3$ g/min and $m_s = 5$ g/min) and without sorbent addition (zeolite 3A). $GHSV = 1250\ h^{-1}$. $P = 1$ atm, other conditions as given in Table 1. (a) $T = 250$ °C, (b) $T = 275$ °C. Different colors indicate conventional or continuous sorbent feeding (CSF) experiments. The different fillings of the blue symbols represent the zeolite mass flow rate. (For interpretation of the references to color in this figure legend, the reader is referred to the web version of this article.)

with continuous zeolite addition. This catalyst exhibits low activity at low temperatures, as shown in Fig. 7.A, where the catalytic activity at 250 °C is nearly negligible. However, increasing the operating temperature to 275 °C (Fig. 7.B) leads to a CO_2 conversion of 6 %, corresponding to approximately one-third of the thermodynamic limit. The high increase in conversion with continuous sorbent feeding (*CSF*) is someway surprising, since being quite far from the thermodynamic equilibrium only a moderate increase in conversion should be expected by the removal of water. These results suggest that, in addition of the reduced reaction rate for water-gas-shift (and therefore increased net reaction rate of CO_2 reduction), the removal of water also avoids a competitive adsorption of water on the catalyst active sites, which would reduce the reaction rate. The presence of a term in the denominator of the reaction rate corresponding to the competitive adsorption of water has been found in many kinetic studies [39–45], but this effect seems to be stronger in the case of the employed catalyst.

When a continuous sorbent feeding (*CSF*) is introduced (blue symbols) and after the time in which sorbent addition starts, marked with vertical lines, a clear increase in CO_2 conversion is observed in all cases, confirming that this novel intensification strategy enhances process efficiency. Notably, this intensification enables increased conversion even at temperatures where the catalyst alone shows limited activity. This is evident in Fig. 7.A, where CO_2 conversion without zeolite is just 0.3 %, but rises to 6 % with continuous zeolite addition—a relative increase of 1500 %. At higher baseline conversions, the relative improvement is smaller, as seen in Fig. 7.B, where conversion increases from 6 % (without zeolite) to 15 % (with zeolite), representing a 250 % increase and achieving 80 % of the thermodynamic equilibrium. The relative enhancement is more pronounced at low conversion levels, probably because the amount of water produced is very low and can be completely adsorbed by the zeolite, allowing the system to operate at its maximum reaction rate. Increasing the operating temperature has two effects: One beneficial and one potentially detrimental. The positive effect is the faster reaction kinetics and a higher thermodynamic limit. The presumed negative effect is the reduced adsorption capacity of the zeolite at higher temperatures. However, in the case of continuous sorbent feeding—as implemented in this study—this reduced capacity is not problematic [24]. Since zeolite is continuously fed and removed from the reactor, the smaller adsorption capacity could be compensated with a larger flow of sorbent. This temperature effect would pose a problem in processes with batch operation of the adsorbent, where the intensification is limited to the "pre-breakthrough" period and ceases once the adsorbent becomes saturated. This limitation is not observed in the present work, as the adsorbent is continuously refreshed, preventing saturation. When the zeolite feed is stopped, the duration of the "pre-breakthrough" period depends on both temperature and conversion. In the low-temperature experiment (250 °C, Fig. 7.A), due to low conversion, the residual zeolite retains adsorption capacity after the feed stops, as the water produced is insufficient to saturate it. Conversely, in the high-temperature experiment (Fig. 7.B), the higher conversion leads to faster saturation of the residual zeolite once feeding ceases, and intensification is no longer sustained.

The reactor setup (Fig. 2) consists of a lateral inlet positioned immediately above the distributor plate and a lateral outlet located 15 cm above the porous support. The inlet enables continuous feeding of regenerated sorbent, carried by a nitrogen stream, while the outlet sets a controlled maximum bed height, facilitating the steady removal of saturated or partially saturated sorbent. The solid exiting the system corresponds exclusively to the upper bed fraction. Under these conditions, effective segregation ensures catalyst retention in the lower section, thereby maintaining a stable catalyst inventory and preserving the Gas Hourly Space Velocity (GHSV). This stability is critical to avoid variations in conversion performance.

Maintaining segregation is thus essential for enabling continuous operation with adsorbent cycling. Regenerated sorbent is introduced into the system, participates in water removal, and is extracted once saturated for ex situ regeneration. This approach offers two main advantages: enhanced intensification through water adsorption and prolonged catalyst lifespan, as the catalyst remains within the reactor and is not subjected to repeated thermal stress associated with regeneration cycles.

Additionally, in order to study the influence of the sorbent addition flow rate m_s, the experiment at 275 °C was repeated with a $m_s = 5$ g/min sorbent addition between minutes 7 and 55. The CO_2 conversion evolution is shown in Fig. 7.B.

Increasing the rate of sorbent addition would imply a greater water adsorption capacity, as a higher amount of sorbent solid would allow more H_2O to be adsorbed. However, this increase in the addition rate does not result in a higher CO_2 conversion compared to the test where a lower but constant amount of sorbent solid was added, at 3 g_{3A}/min. This could be due to two factors: poorer segregation and some elutriation of the catalyst, or the fact that the amount of H_2O formed is lower than what can be adsorbed, meaning the increase in sorbent mass flow would not have a positive effect. Additionally, increasing the sorbent addition rate leads to higher operational costs, as a larger quantity of the solid would be required, as well as more solid to treat for both feeding and subsequent desorption stages.

A parameter to study that has a significant effect is the operating pressure. This is because these variable influences both the reaction kinetics and the thermodynamic equilibrium. An increase in operating pressure enhances reaction kinetics. Additionally, depending on the

specific reaction under study, in methanol synthesis, operating pressure has a significant influence on the thermodynamic equilibrium, enabling the formation of the compound. However, in the case of the reverse water-gas shift (*rWGS*) reaction, the thermodynamic equilibrium is not affected by pressure as described by Le Châtelier's principle.

Fig. 8 illustrates the temporal evolution of CO_2 conversion at the operating temperature that achieved the highest conversion, $T = 275$ °C, with and without the addition of solid sorbent 3 g/min, but under an operating pressure of 20 atm.

At *TOS* = 20 min, the CO_2 conversion is notably higher in the test with the addition of sorbent compared to the test without it, consistent with previous observations in this study. However, the increase in operating pressure results in a reduction in CO_2 conversion (comparing with Fig. 7.B). This decline is attributed to the proportional rise in GHSV caused by the higher pressure. Since CO_2 conversion depends on *GHSV*, lower *GHSV* values result in higher conversion rates due to the longer residence time.

It can also be observed that at *TOS* > 40 min, the CO_2 conversion in the test with the addition of sorbent is lower than the CO_2 conversion obtained in the test without sorbent. This occurs because, in that experiment, the mass of catalyst in the bed decreased as the experiment progressed. Since the zeolite moves in and out of the reactor, it can carry away catalyst particles, leading to a reduction in CO_2 conversion.

While the *rWGS* reaction (5) is not dependent on operating pressure ($\Delta n_g = 0$), methanol synthesis (1) does exhibit such dependence, with the reaction being favored and its thermodynamic equilibrium enhanced under higher pressure. However, due to the high *GHSV*, methanol formation was negligible. As a result, the entirety of the CO_2 conversion is attributed to the RWGS reaction.

A limiting variable in a fluidized bed reactor is the mass flow rate of reactants (total gas flow), as the establishment of this parameter is dependent on the minimum fluidization velocity. This variable is critical because, at velocities below this threshold ($u < u_{mf}$), the particles would not be fluidized. Conversely, at velocities exceeding the critical velocity ($u > u_c$), the particles would be elutriated from the reactor. However, the minimum fluidization velocity depends on several operational parameters: particle size (d_p), solid density (ρ_s), and the density of the feed gas (ρ_g), which in turn depends on *T* (°C), *P* (atm), and gas composition (%^{v}). In this sense, an increase in operating pressure *P* leads to an increase in the minimum fluidization velocity u_{mf} (measured at STP conditions) and, consequently, an increase in the working gas hourly space velocity (*GHSV*). Figs. 7.B and 8 allow to compare the evolution of CO_2 conversion in two experiments without sorbent addition ($m_s = 0$) and different *GHSV* values (1250 and 18,100 h^{-1}). The comparison illustrates the influence of *GHSV* on the *rWGS* reaction (5), whose equilibrium is independent of operating pressure. It can clearly be seen the strong dependence of CO_2 conversion on the *GHSV*, as expected. The increase of operating pressure from 1 to 20 atm, resulting in a 14.5-fold increase in *GHSV*, involves the same qualitative evolution but leads to a noticeable reduction in CO_2 conversion, amounting to around 66 %.

4. Conclusion

The concept of sorption enhanced reaction with continuous sorbent feeding (*CSF*), by segregating a catalyst and a sorbent in a fluidized bed reactor for the methanol synthesis, has been proved. The addition of zeolite 3A in a reactor with In_2O_3/ZrO_2 catalyst favors the correct operation of the system with continuous addition/removal of sorbent, with only small catalyst losses during the tests carried out.

The temperature decreases from 275 to 250 °C supposed a significant worsening of the CO_2 conversion without sorbent addition. However, when sorbent was incorporated to the reactor, this fall was less important which probe that the continuous removal or water from the reactor with the use of zeolite works properly.

Although the CO_2 conversions obtained in this study were not very high (due to the thermodynamic equilibrium of the *rWGS* reaction), operating with a catalyst with higher activity, closer to the equilibrium limit, could result in conversions and productions even surpassing this threshold.

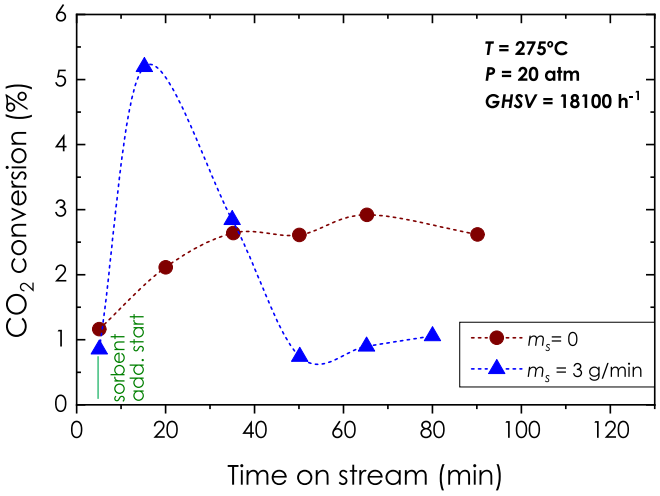

Fig. 8. CO_2 conversion as a function of time-on-stream, with continuous sorbent feeding (*CSF*) (m_s = 3 g/min) (zeolite 3A) and conventional process *T* = 275 °C. *GHSV* = 18,100 h^{-1}. *P* = 20 atm. Other conditions as given in Table 1.

It has been observed that a higher sorbent addition flowrate has produced a negative effect on the CO_2 conversion, inferring the existence of an optimal value of this operating variable, probably because the entrainment of the catalyst with high sorbent flowrate.

Finally, it may be expected that a more active catalyst will allow operation at lower temperature, which would favor water sorption and the positive effect of the sorbent.

CRediT authorship contribution statement

R. González-Pizarro: Writing – original draft, Validation, Conceptualization. **J. Lasobras:** Validation, Investigation, Conceptualization. **J. Soler:** Writing – review & editing, Writing – original draft, Methodology, Conceptualization. **J. Herguido:** Writing – review & editing, Writing – original draft, Methodology, Conceptualization. **M. Menéndez:** Writing – review & editing, Writing – original draft, Supervision, Methodology, Funding acquisition, Conceptualization.

Declaration of competing interest

The authors declare that they have no known competing financial interests or personal relationships that could have appeared to influence the work reported in this paper.

Data availability

No data was used for the research described in the article.

Acknowledgements

Financial support from *Agencia Española de Investigación* (Projects PDC2022-133066-I00/AEI/10.13039/501100011033 and PID2022-139819OB-I00), with financial support from the European Union "NextGeneration EU"/PRTR and European Union Fund for Recovery and Resilience are gratefully acknowledged. Authors would like to acknowledge the use of *Servicio General de Apoyo a la Investigación-SAI, Universidad de Zaragoza*.

References

[1] G. Centi, S. Perathoner, Opportunities and prospects in the chemical recycling of carbon dioxide to fuels, Catal. Today 148 (2009) 191–205, https://doi.org/10.1016/j.cattod.2009.07.075.

[2] G. Centi, E.A. Quadrelli, S. Perathoner, Catalysis for CO_2 conversion: a key technology for rapid introduction of renewable energy in the value chain of chemical industries, Energy Environ. Sci. 6 (2013) 1711–1731, https://doi.org/10.1039/c3ee00056g.

[3] R.J. Detz, J.N.H. Reek, B.C.C. Van Der Zwaan, The future of solar fuels: when could they become competitive? Energy Environ. Sci. 11 (2018) 1653–1669, https://doi.org/10.1039/c8ee00111a.

[4] K. Calvin, D. Dasgupta, G. Krinner, A. Mukherji, P.W. Thorne, C. Trisos, et al., IPCC, 2023: Climate Change 2023: Synthesis Report. Contribution of Working Groups I, II and III to the Sixth Assessment Report of the Intergovernmental Panel on Climate Change [Core Writing Team, H. Lee and J. Romero (eds.)], IPCC, Geneva, Switzerland, 2023, https://doi.org/10.59327/IPCC/AR6-9789291691647.

[5] C. Fuchs, U. Arnold, J. Sauer, Synthesis of sustainable aviation fuels via (co–) oligomerization of light olefins, Fuel 382 (2025), https://doi.org/10.1016/j.fuel.2024.133680.

[6] N. Wulff, D.E. Aliabadi, S. Hasselwander, T. Pregger, H.C. Gils, S. Kronshage, W. Grimme, J. Horst, C. Hoyer-Klick, P. Jochem, Energy system implications of demand scenarios and supply strategies for renewable transportation fuels, Energy Strateg. Rev. 58 (2025), https://doi.org/10.1016/j.esr.2024.101606.

[7] J. van Kampen, J. Boon, F. van Berkel, J. Vente, M. van Sint Annaland, Steam separation enhanced reactions: review and outlook, Chem. Eng. J. 374 (1286–1303) (2019), https://doi.org/10.1016/j.cej.2019.06.031.

[8] R.L. Espinoza, E. Du Toit, J. Santamaria, M. Menendez, J. Coronas, S. Irusta, Use of membranes in Fischer-tropsch reactors, Stud. Surf. Sci. Catal. 130 A (2000) 389–394, https://doi.org/10.1016/s0167-2991(00)80988-x.

[9] Menéndez M. Piera E. Coronas J. Santamaría J. Reactor de membrana zeolítica para la obtención de metanol y otros alcoholes a partir de gas de síntesis. Spanish patent n° ES2164544 2003.

[10] F. Gallucci, L. Paturzo, A. Basile, An experimental study of CO_2 hydrogenation into methanol involving a zeolite membrane reactor, Chem. Eng. Process. Process Intensif. 43 (2004) 1029–1036, https://doi.org/10.1016/j.cep.2003.10.005.

[11] N. Diban, A.T. Aguayo, J. Bilbao, A. Urtiaga, I. Ortiz, Membrane reactors for in situ water removal: a review of applications, Ind. Eng. Chem. Res. 52 (2013) 10342–10354, https://doi.org/10.1021/IE3029625.

[12] M.P. Rohde, D. Unruh, G. Schaub, Membrane application in Fischer-Tropsch synthesis reactors — overview of concepts, Catal. Today 106 (2005) 143–148, https://doi.org/10.1016/j.cattod.2005.07.124.

[13] L.A. da Silva, V. Heczko, M. Schmal, P.H. Cury Camargo, R.M. Brito Alves, R. Giudici, Catalytic and kinetic evaluation of Fe/HZSM-5 catalyst for Fischer-Tropsch synthesis, Chem. Eng. J. 505 (2025), https://doi.org/10.1016/j.cej.2025.159203.

[14] M. Seshimo, et al., Membrane reactor for methanol synthesis using Si-rich LTA zeolite membrane 11 (2021) 505, https://doi.org/10.3390/membranes.

[15] R. Raso, M. Tovar, J. Lasobras, J. Herguido, I. Kumakiri, S. Araki, M. Menéndez, Zeolite membranes: comparison in the separation of $H_2O/H_2/CO_2$ mixtures and test of a reactor for CO_2 hydrogenation to methanol, Catal. Today 364 (2021) 270–275, https://doi.org/10.1016/j.cattod.2020.03.014.

[16] D. Gao, W. Li, H. Wang, G. Wang, R. Cai, Heterogeneous catalysis for CO_2 conversion into chemicals and fuels, Trans. Tianjin Univ. 28 (2022) 245–264, https://doi.org/10.1007/s12209-022-00326-x.

[17] P. Rodriguez-Vega, A. Ateka, I. Kumakiri, H. Vicente, J. Ereña, A.T. Aguayo, J. Bilbao, Experimental implementation of a catalytic membrane reactor for the direct synthesis of DME from H_2+CO/CO_2, Chem. Eng. Sci. 234 (2021), https://doi.org/10.1016/j.ces.2020.116396.

[18] Z. Li, T.T. Tsotsis, Methanol synthesis in a high-pressure membrane reactor with liquid sweep, J. Membr. Sci. 570-571 (2019) 103–111, https://doi.org/10.1016/j.memsci.2018.09.071.

[19] N. Rangnekar, N. Mittal, B. Elyassi, J. Caro, M. Tsapatsis, Zeolite membranes — a review and comparison with MOFs, Chem. Soc. Rev. 44 (2015) 7128–7154, https://doi.org/10.1039/c5cs00292c.

[20] S. Poto, F. Gallucci, M. Fernanda Neira d'Angelo, Direct conversion of CO_2 to dimethyl ether in a fixed bed membrane reactor: influence of membrane properties and process conditions, Fuel 302 (2021), https://doi.org/10.1016/j.fuel.2021.121080.

[21] M. De Falco, M. Capocelli, A. Giannattasio, Membrane reactor for one-step DME synthesis process: industrial plant simulation and optimization, J. CO2 Util. 22 (2017) 33–43, https://doi.org/10.1016/j.jcou.2017.09.008.

[22] Tanaka D. Llosa M. Vittoria M.L. Medrano J.A. Gallucci F. Carbon molecular sieve membrane and its use in separation processes. US patent n° US20220347632A1 2022.

[23] S. Poto, J.G.H. Endepoel, M.A. Llosa-Tanco, D.A. Pacheco-Tanaka, F. Gallucci, M. F. Neira d'Angelo, Vapor/gas separation through carbon molecular sieve membranes: experimental and theoretical investigation, Int. J. Hydrog. Energy 47 (2022) 11385–11401, https://doi.org/10.1016/j.ijhydene.2021.10.155.

[24] A. Borgschulte, N. Gallandat, B. Probst, R. Suter, E. Callini, D. Ferri, Y. Arroyo, R. Erni, H. Geerlings, A. Züttel, Sorption enhanced CO_2 methanation, Phys. Chem. Chem. Phys. 15 (2013) 9620–9625, https://doi.org/10.1039/c3cp51408k.

[25] S. Walspurger, G.D. Elzinga, J.W. Dijkstra, M. Sarić, W.G. Haije, Sorption enhanced methanation for substitute natural gas production: experimental results and thermodynamic considerations, Chem. Eng. J. 242 (2014) 379–386, https://doi.org/10.1016/j.cej.2013.12.045.

[26] J. Terreni, M. Trottmann, T. Franken, A. Heel, A. Borgschulte, Sorption-enhanced methanol synthesis, Energ. Technol. 7 (2019) 1–9, https://doi.org/10.1002/ente.201801093.

[27] P. Maksimov, A. Laari, V. Ruuskanen, T. Koiranen, J. Ahola, Methanol synthesis through sorption enhanced carbon dioxide hydrogenation, Chem. Eng. J. 418 (2021) 129290, https://doi.org/10.1016/j.cej.2021.129290.

[28] K. Wein, T. Kunz, J. Friedland, R. Güttel, Kinetic effect of in situ water adsorption during CO2 hydrogenation: an experimental investigation, Chem. Eng. Sci. 285 (2024) 119537, https://doi.org/10.1016/j.ces.2023.119537.

[29] J. Van Kampen, J. Boon, J. Vente, M. Van Sint Annaland, Sorption enhanced dimethyl ether synthesis under industrially relevant conditions: experimental validation of pressure swing regeneration, React. Chem. Eng. 6 (2021) 244–257, https://doi.org/10.1039/d0re00431f.

[30] L. Gómez, I. Martínez, M.V. Navarro, R. Murillo, Selection and optimisation of a zeolite/catalyst mixture for sorption-enhanced CO_2 methanation (SEM) process, J CO_2 Util 77 (2023), https://doi.org/10.1016/j.jcou.2023.102611.

[31] L. Gómez, I. Martínez, G. Grasa, R. Murillo, Experimental demonstration of a sorption-enhanced methanation (SEM) cyclic process on a lab-scale TRL-3 fixed bed reactor, Chem. Eng. J. 491 (2024), https://doi.org/10.1016/j.cej.2024.151744.

[32] A. Cañada-Barcala, M. Larriba, V.I. Águeda Maté, J.A. Delgado Dobladez, Synthetic natural gas production through biogas methanation using a sorption-enhanced reaction process, Sep. Purif. Technol. 331 (2024), https://doi.org/10.1016/j.seppur.2023.125714.

[33] M. Kuczynski, M.H. Oyevaar, R.T. Pieters, K.R. Westerterp, Methanol synthesis in a countercurrent gas-solid-solid trickle flow reactor. An experimental study, Chem. Eng. Sci. 42 (1987) 1887–1898, https://doi.org/10.1016/0009-2509(87)80135-5.

[34] A. Coppola, F. Massa, P. Salatino, F. Scala, Evaluation of two sorbents for the sorption-enhanced methanation in a dual fluidized bed system, Biomass Convers. Biorefinery 11 (2021) 111–119, https://doi.org/10.1007/s13399-020-00829-4.

[35] M. Menéndez, R. Ciércoles, J. Lasobras, J. Soler, J. Herguido, A preliminary assessment of sorption-enhanced methanol synthesis in a fluidized bed reactor with selective addition/removal of the sorbent, Catalysts 14 (2024), https://doi.org/10.3390/catal14070409.

[36] O. Martin, A.J. Martín, C. Mondelli, S. Mitchell, T.F. Segawa, R. Hauert, C. Drouilly, D. Curulla-Ferré, J. Pérez-Ramírez, Indium oxide as a superior catalyst for methanol synthesis by CO_2 hydrogenation, Angew. Chem. 128 (2016) 6369–6373, https://doi.org/10.1002/ange.201600943.

[37] A.W. Nienow, N.A. Naimer, T. Chiba, Studies of segregation/mixing in fluidised beds of different size particles, Chem. Eng. Commun. 62 (1987) 53–66, https://doi.org/10.1080/00986448708912050.

[38] S. Renda, J. Lasobras, J. Soler, J. Herguido, M. Menéndez, Dependence of the fluidizing condition on operating parameters for sorption-enhanced methanol synthesis catalyst and adsorbent, Catalysts 14 (2024), https://doi.org/10.3390/catal14070432.

[39] F. Nestler, A.R. Schütze, M. Ouda, M.J. Hadrich, A. Schaadt, S. Bajohr, T. Kolb, Kinetic modelling of methanol synthesis over commercial catalysts: a critical assessment, Chem. Eng. J. 394 (2020), https://doi.org/10.1016/j.cej.2020.124881.

[40] G.H. Graaf, E.J. Stamhuis, A.A.C.M. Beenackers, Kinetics of low-pressure methanol synthesis, Chem. Eng. Sci. 43 (1988) 3185–3195, https://doi.org/10.1016/0009-2509(88)85127-3.

[41] T.S. Askgaard, J.K. Norskov, C.V. Ovesen, P. Stoltze, A kinetic model of methanol synthesis, J. Catal. 156 (1995), https://doi.org/10.1006/jcat.1995.1250.

[42] K.M. Vanden Bussche, G.F. Froment, A steady-state kinetic model for methanol synthesis and the water gas shift reaction on a commercial Cu/ZnO/Al_2O_3 catalyst, J. Catal. 161 (1996) 1–10, https://doi.org/10.1006/jcat.1996.0147.

[43] A.Ya. Rozovskii, G.I. Lin, Fundamentals of methanol synthesis and decomposition, Top. Catal. 22 (2003) 137–150, https://doi.org/10.1023/A:1023555415577.

[44] H.W. Lim, M.J. Park, S.H. Kang, H.J. Chae, J.W. Bae, K.W. Jun, Modeling of the kinetics for methanol synthesis using Cu/ZnO/Al_2O_3/ZrO_2 catalyst: influence of carbon dioxide during hydrogenation, Ind. Eng. Chem. Res. 48 (2009) 10448–10455, https://doi.org/10.1021/ie901081f.

[45] T. Kubota, I. Hayakawa, H. Mabuse, K. Mori, K. Ushikoshi, T. Watanabe, M. Saito, Kinetic study of methanol synthesis from carbon dioxide and hydrogen, Appl. Organomet. Chem. 15 (2001) 121–126, https://doi.org/10.1002/1099-0739(200102)15:2<121::aid-aoc106>3.0.co;2-3.